Computers in Biology and Medicine 108 (2019) 85–92

Contents lists available at ScienceDirect

Computers in Biology and Medicine

journal homepage: www.elsevier.com/locate/compbiomed

PSO optimized 1-D CNN-SVM architecture for real-time detection and classification applications

Bhaskar Navaneeth, M. Suchetha*

School of Electronics Engineering, VIT University, Chennai Campus, India

ARTICLE INFO

Keywords:
Convolutional neural network
Support vector machine
Chronic kidney disease
Salivary diagnosis
Particle swarm optimization

ABSTRACT

In this paper, we propose a novel Particle Swarm Optimized (PSO) One-Dimensional Convolutional Neural Network with Support Vector Machine (1-D CNN-SVM) architecture for real-time detection and classification of diseases. The performance of the proposed architecture is validated with a novel hardware model for detecting Chronic Kidney Disease (CKD) from saliva samples. For detecting CKD, the urea concentration in the saliva sample is monitored by converting it into ammonia. The urea on hydrolysis in the presence of urease enzyme produces ammonia. This ammonia is then measured using a semiconductor gas sensor. The sensor response is given to the proposed architecture for feature extraction and classification. The performance of the architecture is optimized by regulating the parameter values using a PSO algorithm. The proposed architecture outperforms current conventional methods, as this approach is a combination of strong feature extraction and classification techniques. Optimal features are extracted directly from the raw signal, aiming to reduce the computational time and complexity. The proposed architecture has achieved an accuracy of 98.25%.

1. Introduction

The main focus of this work is the use of CNN for real-time identification of diseases [1,2]. The SVM classifier is considered as one of the strong classifiers in machine learning [3,4]. In this work, we have used the CNN algorithm along with the SVM classifier for extracting and classifying the features from the raw sensor signal. Different machine learning approaches are available for data classification. Most of the conventional machine learning approaches use separate techniques for feature extraction and classification. The conventional techniques are unsuitable for real-time applications as the computational time is high. The CNN algorithm is different from conventional machine learning algorithms as it avoids the need for a separate feature extraction operation. In this paper, we have proposed a PSO-based CNN-SVM architecture, which is a combination of a strong feature extraction and classification technique. The PSO algorithm is introduced for optimizing the SVM parameters to obtain better classification performance [5,6].

The blood test is the most common method used for detecting diseases. As extracting blood samples is an invasive technique, it is not always considered as the best method. Nowadays, non-invasive disease detection techniques are gaining popularity. Numerous sensors and medical devices are already developed for detecting diseases like diabetes, cancer, etc., from breath, saliva, urine and other body fluids [7–10]. Recent research results show that the saliva test has the potential to replace the commonly used blood test for detecting CKD [11]. The commonly accepted biomarkers for detecting CKD are urea and creatinine [12,13]. Recent studies conducted on salivary diagnosis reveal a positive correlation between urea and creatinine values in saliva and serum [14]. The salivary test can thus be used as an effective replacement for the blood test. In this work, we have developed and used a novel method for detecting CKD by monitoring the urea concentration in saliva. Urea is produced during protein breakdown and is a waste product which is disposed of through urine. As the kidneys do filtering of urea, the amount of urea content in saliva will rise when they are not working properly. Therefore, it is possible to analyze the functioning of the kidneys by monitoring the urea levels in saliva. Various techniques and devices are available for detecting the urea concentration in body fluids. Most of these are laboratory diagnosis techniques based on diacetyl monoxime or enzymatic methods. However, these methods use massive and complex devices like chemical analyzers which are not suitable for real-time applications. In our analysis, we have applied the enzymatic method for converting urea in the saliva sample into ammonia, and the ammonia gas thus produced is measured using an ammonia gas sensor [15].

The rest of this paper is organized as follows. Section 2 describes the

* Corresponding author.
E-mail address: suchetha.m@vit.ac.in (M. Suchetha).

https://doi.org/10.1016/j.compbiomed.2019.03.017
Received 14 September 2018; Received in revised form 17 March 2019; Accepted 18 March 2019

methodology of the work. In Section 3, results are presented along with the performance evaluation. A relevant discussion based on the outcome and importance of the study are delineated in Section 4. Finally, the conclusion of the work is presented in Section 5.

2. Methodology

Two major operations involved in the machine learning techniques are feature extraction and classification. Principal Component Analysis (PCA), Singular Value Decomposition algorithm (SVD) and Linear Discriminant Analysis (LDA) are some of the frequently used feature extraction techniques [16,17]. The major classification algorithms are Decision Tree (DT), K-Nearest Neighbor (KNN), Perceptron, Random Forest and Support Vector Machine [18–20]. The computational time and complexity are high in the traditional methods as they use separate techniques for feature extraction and classification, and therefore they cannot give better performance in real-time applications. In recent times, the CNN algorithm has emerged as an important deep learning technique. It provides better results compared to traditional algorithms when dealing with real-time problems.

In the CNN architecture, feature extraction and feature classification techniques are combined into a single model, thereby, eliminating the need for a separate algorithm for feature extraction [21]. The Two-Dimensional CNN (2-D CNN) architecture is used in numerous applications like computer vision, image recognition, video processing, text classification, etc. [22,23]. The CNN architecture can be modified and applied to 1-D input signals. However, only a few works are available in the literature which explains the capabilities of the 1-D CNN architecture [24–26]. In the proposed architecture, the SVM classifier is integrated with a 1-D CNN algorithm. This classifier can provide improved classification accuracy compared to other classifiers for both linear and non-linear datasets.

2.1. Mathematical modeling of CNN-SVM architecture

The CNN architecture comprises an input layer, convolution and pooling layers and a fully connected classification layer [27]. The convolution layer is the most important part of the CNN architecture. This layer consists of filters or kernels that extend to the whole input. Every unit of this layer gets input from the preceding layer. Convolution between each filter and input produces an input map. This is done by shifting one function and taking the sum of dot products. The convolution of input and kernel is:

$$f_i(n) = x(n)k(1) + x(n-1)k(2) + \ldots + x(0)k(n) \tag{1}$$

$$f_i(n) = \sum_{j=-n}^{n} x(j+1)k(m-j+1) \tag{2}$$

where x represents the input vector with length n, and k is the kernel filter with length m.

Every convolution operation is followed by a pooling layer in the CNN architecture [28]. The pooling layers are used for down-sampling the signal. Max pooling and average pooling approaches are the commonly used pooling techniques. The average pooling operation is used in our analysis as it considers all the input values. In this pooling operation, the input signal will be divided into different pooling segments, and the average value will be computed from each region. The average value from each segment is obtained as:

$$F(n) = \frac{1}{n}\sum_{i=1}^{n} f_i \tag{3}$$

In our analysis, the input is a 1-D signal, and accordingly, a 1-D filter is used for convolution. The operation of the 1-D CNN algorithm is similar to conventional 2-D CNN. The steps involved in forward and back-propagation for the 1-D CNN algorithm are derived from the 2-D CNN algorithm. During forward propagation, the input for a feature signal of layer '*l*' is the convoluted output of previous feature signal in (*l*-1) and the individual filter kernel. The expression for this is given in equation (4), where each l consists of an m^l feature signal. This can be mathematically expressed as:

$$y_k^l = b_k^l + \sum_{j=1}^{m^{l-1}} conv1D(w_{k,j}^l, s_j^{l-1}) \tag{4}$$

where y_k^l is the k^{th} feature signal input, b_k^l is the bias of the k^{th} signal, $w_{k,j}^l$ is the kernel weight from j^{th} feature signal at layer (l-1) to k^{th} signal on the l layer, and s_j^{l-1} is the j^{th} feature signal output on layer (l-1). The output of the k^{th} signal is obtained by applying the activation function to equation (4).

After the convolution and pooling process, a set of reduced features are obtained. These extracted features are then classified for class prediction. The conventional CNN architecture is incorporated with a fully connected Multilayer Perceptron (MLP) layer with an activation function, which performs the classification operation [29,30]. Every neuron in each layer of the network is linked to the neurons in the next layer. The MLP layer consists of input layers, one or more hidden layers and output layers. The output is produced by a combination of weighted inputs on which a sigmoid activation function is applied [31]. The sigmoid function with argument 't' is:

$$A = \frac{1}{1+e^{-t}} \tag{5}$$

The Back-propagation and Gradient descent algorithms are used in the conventional CNN algorithm with MLP for training [32]. A combination of these two algorithms is chosen to adjust the weight of the neurons by calculating the gradient of loss functions. The difference between the estimated output and the actual output is reduced using these techniques. Initially, the Mean Square Error (MSE) is high as the weights and bias are selected randomly [33]. This error is reduced by updating the bias and weights. For training the CNN algorithm, the output error 'E' and its gradient have to be determined. If these are known, then it is possible to estimate the weight during the learning process, so that the error can be reduced.

$$\frac{\partial E}{\partial w_{k,j}^l} = \Delta w_{k,j}^l \tag{6}$$

$$\frac{\partial E}{\partial w_{k,j}^l} = \frac{\partial E}{\partial y_k^l}\frac{\partial y_k^l}{\partial w_{k,j}^l} \tag{7}$$

From equation (4), above equation can be deduced as:

$$\frac{\partial E}{\partial w_{k,j}^l} = \frac{\partial E}{\partial y_k^l} s_j^{l-1} = \frac{\partial E}{\partial y_k^l} A\left(y_j^{l-1}\right) \tag{8}$$

For determining the gradient, $\frac{\partial E}{\partial y_k^l}$ is calculated as:

$$\frac{\partial E}{\partial y_k^l} = \frac{\partial E}{\partial s_k^l}\frac{\partial s_k^l}{\partial y_k^l} = \frac{\partial E}{\partial s_k^l}\frac{\partial}{\partial y_k^l} A(y_k^l) \tag{9}$$

By finding the derivative of the activation function, $\frac{\partial E}{\partial y_k^l}$ can be derived as:

$$\frac{\partial E}{\partial y_k^l} = \frac{\partial E}{\partial s_k^l} A'(y_k^l) \tag{10}$$

For propagating the error back to the previous layer, $\frac{\partial E}{\partial s_j^{l-1}}$ is determined as:

$$\frac{\partial E}{\partial s_j^{l-1}} = \frac{\partial E}{\partial y_k^l}\frac{\partial y_k^l}{\partial s_j^{l-1}} \tag{11}$$

From equation (4), $\frac{\partial y_k^l}{\partial s_j^{l-1}}$ can be obtained as:

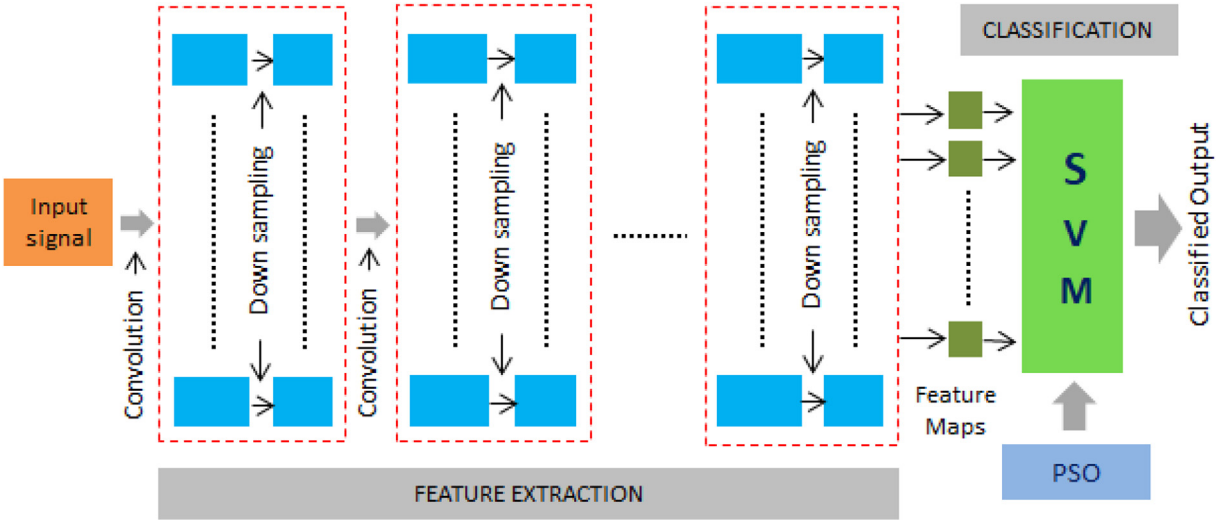

Fig. 1. Architecture of the proposed 1-D CNN-SVM model with PSO.

$$\frac{\partial y_k^l}{\partial s_j^{l-1}} = w_{k,j}^l \tag{12}$$

Finally, the new weights are computed as:

$$w_{k,jnew}^l = w_{k,j}^l + \eta \Delta w_{k,j}^l \tag{13}$$

where η is the learning rate.

The MSE value is calculated as:

$$e_m = \sum (a_i - y_i) \tag{14}$$

where a_i is the actual output and y_i is the estimated output.

The CNN algorithm extracts optimal features from the raw signal but does not always give the best classification performance. Better classification performance can be achieved for the CNN architecture by adopting a powerful classifier like SVM [34]. In the proposed method, the CNN architecture is developed by replacing the last layer with an SVM classifier. The architecture of the proposed model is shown in Fig. 1.

The main concept of the SVM classifier is to isolate the data by defining a hyperplane with maximum margin. The data is labeled in the classifier based on the conditions:

$$x_i w + b > 0,\ c_i = 1 \tag{15}$$

$$x_i w + b < 0,\ c_i = -1 \tag{16}$$

where x represents the input feature vector, w represents the weight vector, b is the bias and c_i is the class label to which the input belongs. The hyperplane is computed by reducing w, and this increases the margin of separation. The optimization problem in the SVM classifier is:

$$minimize \frac{1}{2} \|w\|^2 \tag{17}$$

$$subject\ to\ c_i(x_i w + b) \geq 1 \tag{18}$$

A Gaussian kernel is used in our architecture due to its inherent advantages [35]. The samples are classified based on the decision function:

$$F(x) = \sum_{i=1}^{n} \alpha_i c_i K(x_i, x) + b \tag{19}$$

where $K(x_i, x)$ represents the kernel function, and α represents the Lagrange multiplier.

2.2. PSO optimization in the proposed architecture

The architecture is optimized by implementing a PSO algorithm. We have used this algorithm for tuning and selecting the regularization parameter 'C' and the Gaussian kernel parameter 'γ' [36,37]. The kernel parameter is calculated using the following equation:

$$\gamma = \frac{1}{2\sigma^2} \tag{20}$$

where σ represents the kernel width.

The PSO algorithm is an evolutionary method based on the social behavior of fish schooling or bird flocking. The steps involved in this algorithm are explained in Algorithm 1. Each particle is characterized by its position, velocity and fitness values. The position and velocity of the i^{th} particle in the D-dimensional space are represented as:

$$Z_i = [z_{i1}, z_{i2}, ...,z_{iD}] \tag{21}$$

$$V_i = [v_{i1}, v_{i2}, ...,v_{iD}] \tag{22}$$

Algorithm 1. PSO Algorithm

Algorithm 1 PSO Algorithm

Steps:
1: Initialize the particles.
2: Initialize the current position of particle z_p.
3: Initialize the velocity of the particle v_p.
4: Update the best position.
for $i = 1, 2, ...n$
if $f(z_p) < f(X_i)$ then
$X_i = z_p$
end if
5: Update the global best position of the particle.
if $f(X_i) < f(X_g)$ then
$X_g = X_i$
end if
end for
6: Update the velocity v_{id}^{t+1} of the particle.
7: Update the position of the particle z_{id}^{t+1}.
8: Continue till the termination criterion is satisfied.
end

The individual position of the particle is tracked and updated with respect to personal best position (X_i) and global best position (X_g). The velocity and position are updated as:

$$v_{id}^{t+1} = wv_{id}^t + c_1 r_1 (x_{id}^t - z_{id}^t) + c_2 r_2 (x_{gd}^t - z_{id}^t) \tag{23}$$

$$z_{id}^{t+1} = z_{id}^t + v_{id}^{t+1} \tag{24}$$

where w represents the inertia factor, t is the number of iterations, c_1 and c_2 are the positive constants for regulating the velocities and r_1 and r_2 are the uniformly distributed random variables in the range [0, 1].

The stopping criterion is the movement of the particle beyond the specified boundaries of the search limit. This is achieved by prefixing the particle position and by changing the search direction. This prevents the particle from crossing the search space. The inertia factor is chosen as 0.45, and the swarm size is set as 50. The values of c_1 and c_2 are set as 1. The endpoints of the searching window of parameter C are set as [0.01 and 1000]. Similarly, the searching range for γ is set as [0.001, 10] [6]. The fitness of each particle is determined after each step to find the optimal value. The SVM classifier is retrained after obtaining the optimized parameters.

2.3. Sample collection

The experimental study has been carried out by collecting samples from 104 participants, which include 40 healthy individuals and 64 chronic kidney patients. The participants have been informed about the purpose and importance of the study. Prior to the sample collection, they have cleaned their mouth using distilled water to maintain oral hygiene. 2 ml of saliva has been collected using spitting method in a sterile test tube with their consent. The sample collection and clinical validation have been carried out at the Community Health Center and the experimental testing and simulation at the Signal Processing Laboratory. This research work has been performed by following the principles of the Declaration of Helsinki.

2.4. Sensing unit

The hardware section of the proposed model consists of an ammonia gas sensor, a gas sensing chamber and an Arduino Uno SMD R3 board. Fig. 2 shows the snapshot of the experimental setup. The sensor arrangement is mounted inside the gas chamber. An MQ 137 series gas sensor, which is highly sensitive to ammonia gas, is used for the analysis. The sensitive layer of tin dioxide on the sensor is responsible for ammonia detection. The schematic of the detection circuit with the sensor is shown in Fig. 3. A load resistance of 47 KΩ is used in the circuit. The sensor circuit requires a circuit voltage for providing the detection voltage to the sensor. It also requires a heater voltage for providing the working temperature. Before the analysis, the sensor has been tested to study its response for varying concentrations of ammonia gas. When the urea component in saliva comes in contact with urease enzyme, hydrolysis of urea takes place. During this process, the urea is converted into ammonia gas. This is based on the principle of the conventional enzymatic method of urea detection [15]. For our experimentation, we have placed enough amount of urease enzyme required for this conversion process in a beaker below the inlet valve, inside the gas chamber. The saliva sample is dropped into this beaker using a microsyringe through the inlet valve. Depending on the ammonia gas produced inside the chamber, the conductivity of the sensor increases. This change in conductivity is converted into an analog voltage. The output response of the sensor is obtained through the Arduino Uno board. Fig. 4 shows the voltage response of the gas sensor for a healthy subject's sample.

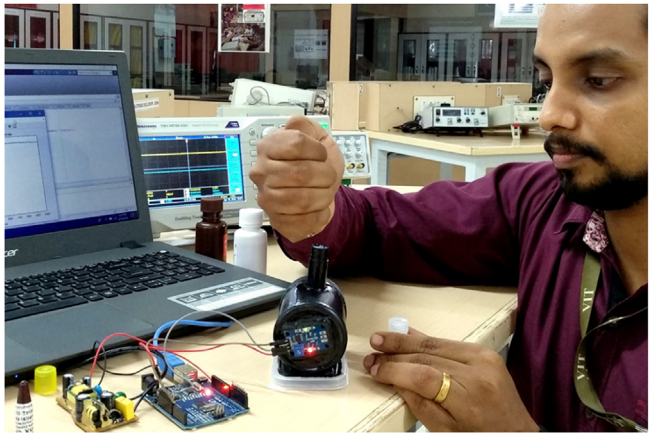

Fig. 2. Snapshot of the test setup and experimentation. The saliva sample is dropped through the inlet valve of the gas chamber, which has an ammonia sensor embedded in it. The sensor circuit is interfaced with the Arduino Uno board.

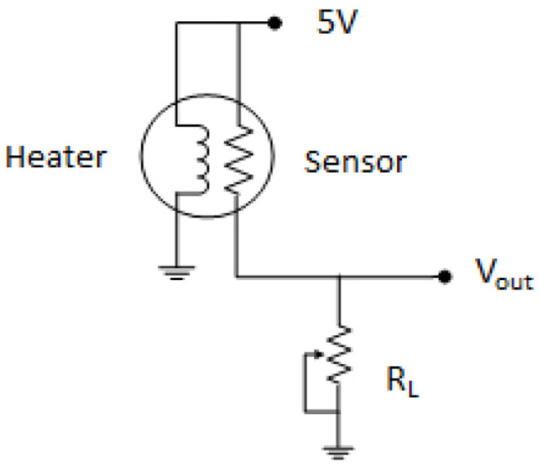

Fig. 3. Schematic of detection circuit with sensor.

3. Results

As we have used a novel sensing technique, the sensor has been tested for studying its response to varying concentrations of ammonia gas. From the experimental study, it is observed that the maximum voltage of the sensor response is in the range of 0.62–0.93 V for healthy individuals, and the values are above 0.93 V for kidney patients. This separation in voltage range is due to the increase in urea concentration in saliva of CKD patients. The ammonia concentration has been measured using an MQ 137 series sensor [38,39]. These values are used as the reference levels for classifying healthy subjects and CKD patients. The output of the sensory device is given to the learning algorithm for analysis. The processes carried out in our proposed method are shown in Fig. 5. For analysing the performance of the proposed PSO-optimized

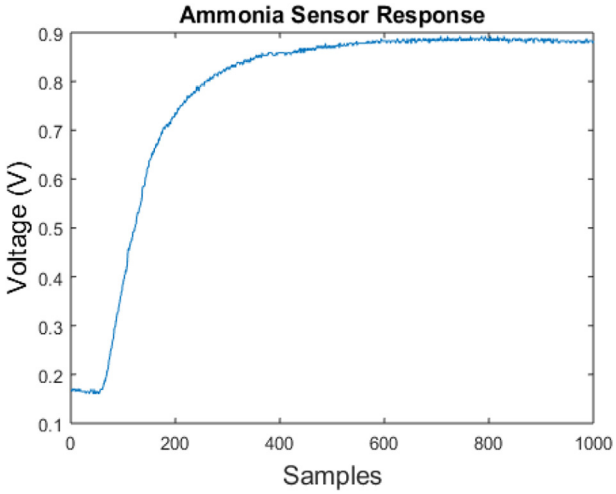

Fig. 4. Sensor response of a healthy subject.

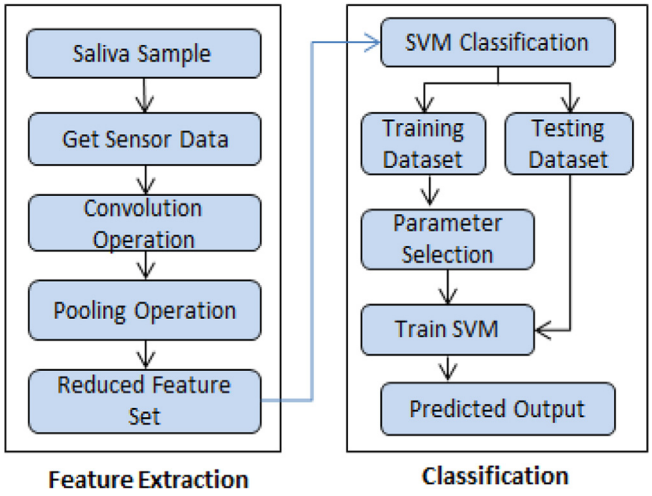

Fig. 5. Computational flow of the entire process.

1-D CNN-SVM architecture, we have implemented a conventional SVM algorithm with handpicked features and a conventional 1-D CNN with fully connected MLP layer and tested them with the same sensor response. The simulation is done in Matlab 9.2 environment.

3.1. Performance evaluation of conventional SVM

Initially, the signals obtained from the sensor are processed through the SVM classifier with handpicked features. The classifier is programmed to categorize the feature sets as 'Healthy' and 'Abnormal' samples. The Matlab function *svmtrain* is used to train the classifier. The classifier is trained with 30% of the sample sets. After the training, the samples are tested and classified using the function *svmclassify*. The classification is done based on the decision function:

$$F(x) = \sum_{i=1}^{n} \alpha_i c_i(x_i, x) + b \tag{25}$$

Two features are extracted from the sensor response for classification. They are maximum output voltage and area under the response curve. Fig. 6 shows the output of the SVM classifier. The classifier has successfully classified the samples as 'Healthy' and 'Abnormal' with an accuracy of 95.61%.

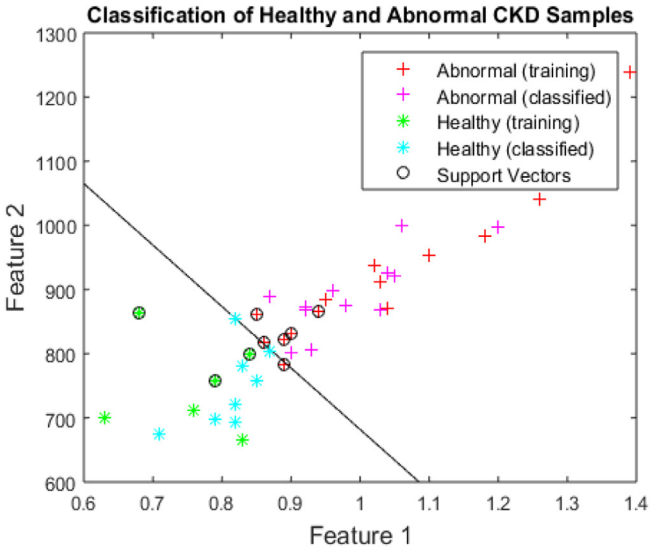

Fig. 6. Classification of samples using the SVM classifier with linear kernel.

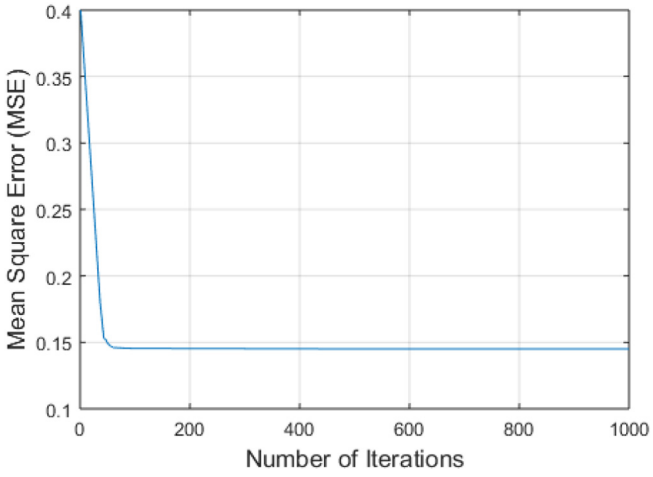

Fig. 7. Mean square error plot.

3.2. Performance evaluation of conventional 1-D CNN with MLP

For the comparison purpose, we have implemented a conventional 1-D CNN model with MLP. The raw signal from the ammonia sensor is directly given to the CNN architecture. Initially, the input signals are convoluted with the kernel function. We have used 1-D kernels with different sizes for convolution in each layer. The kernel size is derived through trial and error method [1]. As the dimensions of the convoluted signal are large, it is reduced using the pooling operation. A sliding 1-D window is used for dividing the feature maps into multiple segments, and the mean value is extracted from each segment.

The down-sampled signals are given to the MLP layer for classification. The number of neurons in the hidden layers are selected as 20 [21]. For reducing the classification error, the initial weights that are chosen randomly are updated using an iterative method. The number of iteration count is set as 1000 with a learning rate of 0.001. With each iteration, the mean square error decreases. The performance of conventional CNN architecture is evaluated using the Leave-One-Out validation process [40]. The MSE value has been reduced to 0.152 after successive iterations as shown in Fig. 7. The conventional CNN algorithm with MLP achieved an accuracy, specificity and sensitivity of 96.49%, 95.24% and 98.04% respectively.

3.3. Performance evaluation of the proposed architecture

In the MLP algorithm, the learning is based on minimizing the error. The optimal values for the weights are obtained by reducing the error function. In the proposed architecture, we have replaced the MLP layer in the conventional CNN architecture with the SVM classifier. The initial steps are the same as in conventional CNN, where the optimal features are obtained by passing the signal through convolution and pooling layers.

The proposed architecture is implemented with four convolution and pooling layers. The dimension of the input signal is 1×1000. First, the input is convoluted with a kernel. The convoluted signal is then down-sampled using average pooling operation to reduce the dimensions of the feature map. We have applied an average pooling of size two to every feature map. Convolution and pooling operations are repeated to get the reduced feature map. After successive convolution and pooling operations, the size of the feature set is reduced to 1×4. These features are then given to the SVM classifier for classification and disease detection. As mentioned earlier, the SVM classifier separates the data into different classes based on the hyperplane. In this work, we have used the SVM classifier with a Gaussian kernel. The classification function of the kernel is:

$$F(x) = \sum_{i=1}^{n} \alpha_i c_i exp\frac{(-\|x_i - x\|^2)}{2\sigma^2} + b \quad (26)$$

In the proposed architecture, optimal values of C and γ are selected using the PSO algorithm. This gives better classification accuracy than using default parameter values. The classification is performed using the SVM classifier, and the fitness function is determined for every particle p_i (i = 1, 2,…, n). The best position X_i of the particle is updated if the current position x_i (i = 1, 2,…, n) has a lower value for the fitness function. The global best position X_g is chosen in swam, and the classifier is trained with X_g mapped features. The SVM classifier is modeled with the kernel parameter and cost function values at identical positions. The introduction of PSO improved the performance of the classifier by choosing the optimum values of the parameters.

3.4. Evaluation and comparison of performance parameters

The proposed architecture is trained and tested for various sensor outputs. For validating the stability of the model, a ten-fold cross-validation process is carried out [41]. This is done by dividing the data into ten subsamples. One of the subsamples is kept as the test sample, and the remaining nine subsamples are used as the training set. This is repeated for all the samples, and the performance parameters are calculated for each iteration. Finally, the average value is taken to find the overall performance of the system.

Apart from the proposed model, the same sensor output has been analyzed using the conventional linear SVM algorithm and the conventional CNN algorithm for performance evaluation and comparison. The commonly used classification performance parameters are computed for evaluation. The values obtained for different algorithms are presented in Table 1. The proposed architecture has achieved an accuracy of 98.25%. The values obtained for sensitivity and specificity are 98.04% and 98.41% respectively. The sensitivity is the proportion of getting a positive test result when the disease is present, and the specificity is the proportion of getting a negative result when the disease is not present. The precision of 0.984 for the proposed architecture specifies that 98.4% of participants who are diagnosed with CKD are in fact affected by the disease. The False Positive Rate (FPR) is the proportion of all normal cases that are classified as CKD, whereas the False Negative Rate (FNR) is the proportion of all CKD subjects that are classified as normal. The False Discovery Rate (FDR) is the number of normal cases wrongly classified as CKD out of all the subjects classified as CKD. The lower values of FPR, FNR and FDR obtained for the proposed architecture indicate the effectiveness of the algorithm. The Negative Predictive Value (NPV) is the proportion of all the normal cases that are truly normal.

The F1 score and Matthews Correlation Coefficient (MCC) are different measures of accuracy. The F1 score is the weighted average of precision and sensitivity. The MCC value gives a balanced measure as it considers all the elements of the confusion matrix. It is considered as one of the best measures as it describes the whole confusion matrix by a single value. F1 score and MCC are determined using the following equations:

$$F1\ score = \frac{2 \times P_T}{2 \times P_T + N_F + P_F} \quad (27)$$

$$MCC = \frac{P_T \times N_T - P_F \times N_F}{\sqrt{(P_T + P_F)(P_T + N_F)(N_T + P_F)(N_T + N_F)}} \quad (28)$$

where P_T, P_F, N_T and N_F represent the True Positive, False Positive, True Negative and False Negative values respectively.

Table 1
Performance evaluation of different techniques.

Performance Parameters	Conventional SVM	CNN-MLP	Proposed Architecture
Accuracy (%)	95.61	96.49	98.25
Sensitivity (%)	98.03	98.04	98.04
Specificity (%)	93.65	95.24	98.41
Precision	0.926	0.943	0.984
FPR	0.063	0.048	0.015
FNR	0.02	0.019	0.019
NPV	0.983	0.984	0.984
FDR	0.074	0.057	0.019
F1 Score	0.952	0.962	0.981
MCC	0.913	0.929	0.964

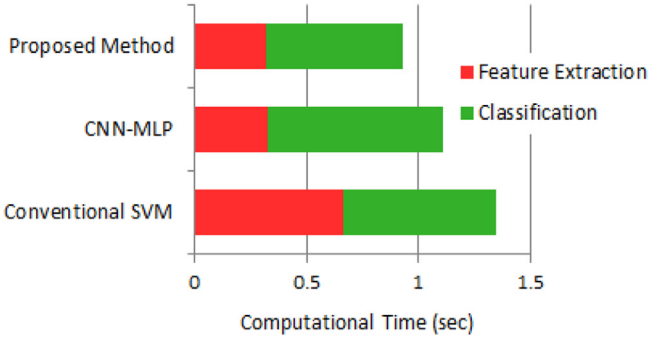

Fig. 8. Comparison of computational time of different algorithms.

The computational time taken by different algorithms for execution is represented in Fig. 8. Overall simulation time is the total time taken for feature extraction and classification. As the features are extracted directly from the raw signals, the CNN-based model takes relatively less time compared to the conventional SVM classifier. The time taken for execution by the proposed algorithm is 0.9283s. This is relatively less compared to the conventional SVM algorithm and CNN-MLP algorithm.

The Receiver Operating Characteristic (ROC) curve is plotted for the proposed architecture to find the diagnostic ability of the analysis to differentiate healthy and chronic kidney patients [42]. It is the sketch of sensitivity across 1-specificity for numerous cutoff points of the test values. The ROC plot of the analysis is shown in Fig. 9. From this plot, the Area Under the Curve (AUC) is determined for checking the accuracy of the analysis. The AUC values achieved are 0.981 and 0.978 for healthy and abnormal samples respectively.

3.5. Clinical validation

To validate the analysis results, clinical validation is conducted by monitoring the Glomerular Filtration Rate (GFR) of the participants [43]. The GFR value specifies the rate at which the kidney is filtering waste products. For a healthy person, GFR will be more than 90 mL/

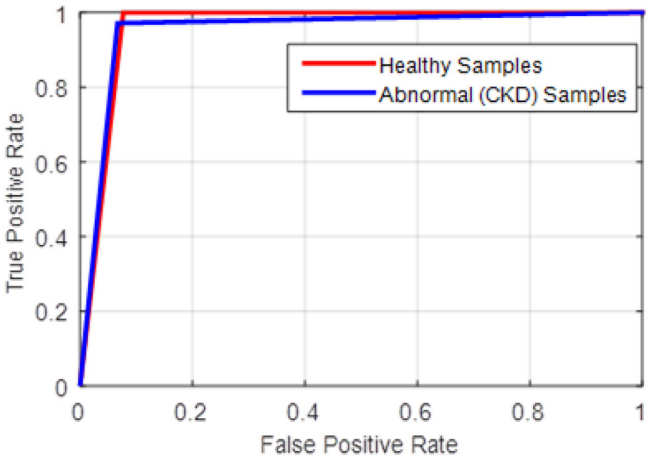

Fig. 9. ROC plot of the analysis.

min. We have chosen this method as a measure for validation as it is one of the most widely accepted methods to diagnose kidney disease. The GFR value is determined based on the blood creatinine test, age, body size and gender. This test is done with the aid of health professionals at the Community Health Center. The test results are validated by a clinician. The results obtained through the analysis and the clinical evaluation results have a minimum difference with less than 2% of deviation. This shows that the proposed method is more effective for detecting CKD non-invasively.

4. Discussion

The conventional machine-learning approaches use separate techniques for feature extraction and classification. For real-time analysis of signals, these techniques are not appropriate as the computational time and complexity are more. The CNN algorithm nullifies the need for a separate algorithm for extracting features from the sensor response. While we have a good number of contemporary research papers that explain the capabilities of 2-D CNN, very few focus on 1-D CNN [21,24,25,27,44]. An algorithm presented by Kiranyaz et al. [21] demonstrates the use of the 1-D CNN algorithm for analyzing real-time ECG signals. In a recent work by Lekha et al. [24], a novel architecture is proposed for real-time detection of diabetes using 1-D CNN. In this paper, the authors have implemented the 1-D CNN architecture by modifying the conventional CNN architecture. Ince et al. [25] have used the 1-D CNN architecture for real-time fault detection in motors. In addition, a study conducted by Zhang et al. [44] reports the use of CNN for classification of physiological data. The above-mentioned works suggest that the CNN architecture can be adapted and applied for 1-D input signals.

In this work, we have developed an innovative 1-D CNN-SVM architecture for real-time detection and classification of CKD. A novel sensing model capable of detecting CKD from the saliva sample is developed for testing the proposed architecture. The latest researches in medical testing are focused on developing non-invasive techniques as they are gaining popularity. Urine, saliva, breath and sweat are the most commonly used samples for non-invasive diagnosis. For detecting CKD non-invasively, urine is the only used test sample. The salivary test can be used as a reliable alternative to the urine test for non-invasive CKD detection. The saliva-based diagnosis is advantageous as the sample collection is hassle-free and cause less discomfort to patients. Thus, it is acceptable to patients of all age groups as well as genders.

The urea is considered as one of the effective biomarkers for detecting kidney disease. There are various methods available for detecting urea concentration. In this work, the urea in the saliva sample is converted into ammonia, which is detected by the developed sensor. The breath-based analysis is also an option to detect CKD non-invasively as it contains ammonia [38,39]. However, the level of ammonia concentration is low in human breath, which makes the detection process difficult. It demands highly sensitive sensors to measure the minute concentration of ammonia. This limitation makes breath-based analysis more complex compared to saliva-based diagnosis.

We have used the SVM classifier along with the CNN architecture, for classifying the extracted features and for making decisions. The CNN-based models are found to perform better than the conventional SVM algorithm. The performance of the conventional CNN architecture has improved when MLP is substituted by the SVM classifier. This finding is in agreement with the results published by Wu et al. [45]. They have reported that the CNN-SVM combined model improved the classification accuracy, as it makes use of the advantages of both CNN and SVM. In a work published by Lekha et al. [27], the authors have developed an architecture by integrating the SVM classifier with conventional CNN for addressing the shortcomings of MLP and improving the overall performance. The CNN algorithm helps to improve the performance by automatically extracting the discriminant features from the signal. The SVM classifier has better generalization ability and can reduce the computational complexity. The observations of our study and the previously published works show that the CNN-SVM combined model can perform better in real-time applications.

The PSO algorithm is seen applied with the SVM classifier to optimize the classifier performance in a few published works [5,46]. The distinguishing factor in the proposed work is the introduction of PSO in a 1-D CNN-SVM combined model. As per our knowledge, this is the first case where a PSO-optimized CNN-SVM architecture is implemented for analyzing 1-D signals. We have introduced the PSO algorithm to enhance the classifier performance. It automatically solves the model selection by evaluating the optimal values of the kernel parameter and regularization parameter. The PSO-based CNN-SVM architecture has achieved the best performance compared to other techniques. Results show that the use of the PSO algorithm improves the classification accuracy. The computational time is also evaluated in this study. The proposed architecture has taken a total computational time of 0.928s for execution, which is less when compared to the conventional techniques. In addition to evaluating the performance parameters, we have evaluated the ROC plot to ascertain the diagnostic ability of the model. We have achieved a high value for AUC, and this proves the effectiveness of our algorithm.

5. Conclusion

In this work, we have proposed a novel 1-D CNN-SVM architecture which is optimized using a PSO algorithm for real-time detection of CKD non-invasively. The urea concentration in the saliva sample is monitored to detect CKD. In this study, saliva has been chosen as the diagnostic tool as the sample collection method is non-invasive, and the technique is hassle-free. The proposed architecture has obtained maximum accuracy compared to conventional techniques. The addition of the PSO algorithm in the architecture has further improved the classification accuracy. We have carried out experiments on the architecture with the developed hardware model and clinically validated the results. The raw signals obtained from the sensor have been successfully classified with an accuracy, specificity and sensitivity of 98.25%, 98.41% and 98.04% respectively. The proposed architecture has outperformed conventional techniques in terms of accuracy, computational speed and other performance metrics. The proposed approach can be applied for any real-time sensing application with the help of appropriate sensors.

Conflicts of interest

The authors declare that they have no conflict of interest.

Acknowledgement

The authors would like to thank all the participants for their effort and time and the medical team at the Community Health Center, Kannur for their cooperation and support for our research.

This research work did not receive any grant from any funding agencies in the public, commercial, or not-for-profit sectors.

References

[1] U.R. Acharya, S.L. Oh, Y. Hagiwara, J.H. Tan, H. Adeli, Deep convolutional neural network for the automated detection and diagnosis of seizure using eeg signals, Comput. Biol. Med. 100 (2018) 270–278.
[2] bozkurt 2018 study, B. Bozkurt, I. Germanakis, Y. Stylianou, A study of time-frequency features for cnn-based automatic heart sound classification for pathology detection, Comput. Biol. Med. 100 (2018) 132–143.
[3] H.-T. Shiao, V. Cherkassky, J. Lee, B. Veber, E.E. Patterson, B.H. Brinkmann, G.A. Worrell, Svm-based system for prediction of epileptic seizures from ieeg signal, IEEE Trans. Biomed. Eng. 64 (2017) 1011–1022.
[4] D. Lin, L. Sun, K.-A. Toh, J.B. Zhang, Z. Lin, Biomedical image classification based on a cascade of an svm with a reject option and subspace analysis, Comput. Biol. Med. 96 (2018) 128–140.
[5] A. Subasi, Classification of emg signals using pso optimized svm for diagnosis of neuromuscular disorders, Comput. Biol. Med. 43 (2013) 576–586.

[6] S. Raj, K.C. Ray, Ecg signal analysis using dct-based dost and pso optimized svm, IEEE Trans. Instrum. Measur. 66 (2017) 470–478.
[7] C.S. Miller, J.D. Foley, A.L. Bailey, C.L. Campell, R.L. Humphries, N. Christodoulides, P.N. Floriano, G. Simmons, B. Bhagwandin, J.W. Jacobson, et al., Current developments in salivary diagnostics, Biomark. Med. 4 (2010) 171–189.
[8] R.S. Malon, S. Sadir, M. Balakrishnan, E.P. Córcoles, Saliva-based biosensors: noninvasive monitoring tool for clinical diagnostics, BioMed Res. Int. (2014) 2014.
[9] S. Chojnowska, T. Baran, I. Wilińska, P. Sienicka, I. Cabaj-Wiater, M. Knaś, Human saliva as a diagnostic material, Adv. Med. Sci. 63 (2018) 185–191.
[10] M.A. Javaid, A.S. Ahmed, R. Durand, S.D. Tran, Saliva as a diagnostic tool for oral and systemic diseases, J. Oral Biol. Craniof. Res. 6 (2016) 67–76.
[11] P. Celec, L. Tóthová, K. Šebeková, L. Podracká, P. Boor, Salivary markers of kidney function-potentials and limitations, Clin. Chim. Acta 453 (2016) 28–37.
[12] T.J. Lasisi, Y.R. Raji, B.L. Salako, Salivary creatinine and urea analysis in patients with chronic kidney disease: a case control study, BMC Nephrol. 17 (2016) 10.
[13] B.S. Bagalad, K. Mohankumar, G. Madhushankari, M. Donoghue, P.H. Kuberappa, Diagnostic accuracy of salivary creatinine, urea, and potassium levels to assess dialysis need in renal failure patients, Dent. Res. J. 14 (2017) 13.
[14] R. Renda, Can salivary creatinine and urea levels be used to diagnose chronic kidney disease in children as accurately as serum creatinine and urea levels? a case–control study, Ren. Fail. 39 (2017) 452–457.
[15] J. Georges, Determination of ammonia and urea in urine and of urea in blood by use of an ammonia-selective electrode, Clin. Chem. 25 (1979) 1888–1890.
[16] W. Yang, Y. Si, D. Wang, B. Guo, Automatic recognition of arrhythmia based on principal component analysis network and linear support vector machine, Comput. Biol. Med. 101 (2018) 22–32.
[17] O. Nasario-Junior, P.R. Benchimol-Barbosa, G. Trevizani, M. Marocolo, J. Nadal, Effect of aerobic conditioning on ventricular activation: a principal components analysis approach to high-resolution electrocardiogram, Comput. Biol. Med. 43 (2013) 1920–1926.
[18] J. Park, K. Kang, Pchd: personalized classification of heartbeat types using a decision tree, Comput. Biol. Med. 54 (2014) 79–88.
[19] F. Tetschke, U. Schneider, E. Schleussner, O.W. Witte, D. Hoyer, Assessment of fetal maturation age by heart rate variability measures using random forest methodology, Comput. Biol. Med. 70 (2016) 157–162.
[20] A.A. Suárez-León, C. Varon, R. Willems, S. Van Huffel, C.R. Vázquez-Seisdedos, T-wave end detection using neural networks and support vector machines, Comput. Biol. Med. 96 (2018) 116–127.
[21] S. Kiranyaz, T. Ince, M. Gabbouj, Real-time patient-specific ecg classification by 1-d convolutional neural networks, IEEE (Inst. Electr. Electron. Eng.) Trans. Biomed. Eng. 63 (2016) 664–675.
[22] T. Zhou, G. Han, B.N. Li, Z. Lin, E.J. Ciaccio, P.H. Green, J. Qin, Quantitative analysis of patients with celiac disease by video capsule endoscopy: a deep learning method, Comput. Biol. Med. 85 (2017) 1–6.
[23] W.B. Sampaio, E.M. Diniz, A.C. Silva, A.C. De Paiva, M. Gattass, Detection of masses in mammogram images using cnn, geostatistic functions and svm, Comput. Biol. Med. 41 (2011) 653–664.
[24] S. Lekha, M. Suchetha, Real-time non-invasive detection and classification of diabetes using modified convolution neural network, IEEE J. Biomed. Health Inf. 22 (2018) 1630–1636.
[25] T. Ince, S. Kiranyaz, L. Eren, M. Askar, M. Gabbouj, Real-time motor fault detection by 1-d convolutional neural networks, IEEE Trans. Ind. Electron. 63 (2016) 7067–7075.
[26] S.H. Choi, H. Yoon, H.S. Kim, H.B. Kim, H.B. Kwon, S.M. Oh, Y.J. Lee, K.S. Park, Real-time apnea-hypopnea event detection during sleep by convolutional neural networks, Comput. Biol. Med. 100 (2018) 123–131.
[27] S. Lekha, M. Suchetha, A novel 1-d convolution neural network with svm architecture for real-time detection applications, IEEE Sens. J. 18 (2018) 724–731.
[28] Y. Miki, C. Muramatsu, T. Hayashi, X. Zhou, T. Hara, A. Katsumata, H. Fujita, Classification of teeth in cone-beam ct using deep convolutional neural network, Comput. Biol. Med. 80 (2017) 24–29.
[29] I. Güler, E.D. Übeyli, Detection of ophthalmic arterial Doppler signals with behcet disease using multilayer perceptron neural network, Comput. Biol. Med. 35 (2005) 121–132.
[30] F.-L. Chung, S. Wang, Z. Deng, D. Hu, Catsmlp: toward a robust and interpretable multilayer perceptron with sigmoid activation functions, IEEE Trans. Syst., Man Cybern. B (Cybernetics) 36 (2006) 1319–1331.
[31] S.M. Siniscalchi, V.M. Salerno, Adaptation to new microphones using artificial neural networks with trainable activation functions, IEEE Trans. Neural Netw. Learn. Syst. 28 (2017) 1959–1965.
[32] D. Erdogmus, O. Fontenla-Romero, J.C. Principe, A. Alonso-Betanzos, E. Castillo, Linear-least-squares initialization of multilayer perceptrons through back-propagation of the desired response, IEEE Trans. Neural Netw. 16 (2005) 325–337.
[33] M.S. Salman, O. Kukrer, A. Hocanin, Recursive inverse algorithm: mean-square-error analysis, Digit. Signal Process. 66 (2017) 10–17.
[34] M. Elleuch, R. Maalej, M. Kherallah, A new design based-svm of the cnn classifier architecture with dropout for offline Arabic handwritten recognition, Procedia Comput. Sci. 80 (2016) 1712–1723.
[35] R. Ahmed, A. Temko, W.P. Marnane, G. Boylan, G. Lightbody, Exploring temporal information in neonatal seizures using a dynamic time warping based svm kernel, Comput. Biol. Med. 82 (2017) 100–110.
[36] E. Abbasi, M. Ghatee, M.E. Shiri, Fran and rbf-pso as two components of a hyper framework to recognize protein folds, Comput. Biol. Med. 43 (2013) 1182–1191.
[37] A. Gudigar, U. Raghavendra, T.R. San, E.J. Ciaccio, U.R. Acharya, Application of multiresolution analysis for automated detection of brain abnormality using mr images: a comparative study, Future Gener. Comput. Syst. 90 (2019) 359–367.
[38] T. Saidi, O. Zaim, M. Moufid, N. El Bari, R. Ionescu, B. Bouchikhi, Exhaled breath analysis using electronic nose and gas chromatography–mass spectrometry for non-invasive diagnosis of chronic kidney disease, diabetes mellitus and healthy subjects, Sensor. Actuator. B Chem. 257 (2018) 178–188.
[39] T. Jayasree, M. Bobby, S. Muttan, Sensor data classification for renal dysfunction patients using support vector machine, J. Med. Biol. Eng. 35 (2015) 759–764.
[40] T.-T. Wong, Performance evaluation of classification algorithms by k-fold and leave-one-out cross validation, Pattern Recogn. 48 (2015) 2839–2846.
[41] G. Jiang, W. Wang, Error estimation based on variance analysis of k-fold cross-validation, Pattern Recogn. 69 (2017) 94–106.
[42] A. Fernández, L. de Santiago, R. Blanco, C. Pérez-Rico, J. Rodríguez-Ascariz, R. Barea, J.M. Miguel-Jiménez, J. García-Luque, M.O. del Castillo, E.M. Sánchez-Morla, et al., Filtering multifocal vep signals using pronys method, Comput. Biol. Med. 56 (2015) 13–19.
[43] D.K. Ng, G.J. Schwartz, B.A. Warady, S.L. Furth, A. Muñoz, Relationships of measured iohexol gfr and estimated gfr with ckd-related biomarkers in children and adolescents, Am. J. Kidney Dis. 70 (2017) 397–405.
[44] J. Zhang, S. Li, R. Wang, Pattern recognition of momentary mental workload based on multi-channel electrophysiological data and ensemble convolutional neural networks, Front. Neurosci. 11 (2017) 310.
[45] H. Wu, Q. Huang, D. Wang, L. Gao, A cnn-svm combined model for pattern recognition of knee motion using mechanomyography signals, J. Electromyogr. Kinesiol. 42 (2018) 136–142.
[46] M.-Y. Cho, T.T. Hoang, Feature selection and parameters optimization of svm using particle swarm optimization for fault classification in power distribution systems, Comput. Intell. Neurosci. 2017 (2017).